Bulletin of the Seismological Society of America, Vol. 93, No. 3, pp. 1034–1050, June 2003

Fault Structure Control on Fault Slip and Ground Motion during the 1999 Rupture of the Chelungpu Fault, Taiwan

by Richard Heermance,* Zoe K. Shipton,† and James P. Evans

Abstract The Chelungpu fault, Taiwan, ruptured in a M_w 7.6 earthquake on 21 September 1999, producing a 90-km-long surface rupture. Analysis of core from two holes drilled through the fault zone, combined with geologic mapping and detailed investigation from three outcrops, define the fault geometry and physical properties of the Chelungpu fault in its northern and southern regions. In the northern region the fault dips 45°–60° east, parallel to bedding in both the hanging wall and footwall, and consists of a narrow (1–20 cm) core of dark gray, sheared clay gouge. The gouge is located at the base of a 30- to 50-m zone of increased fracture density confined asymmetrically to the hanging wall. Microstructural analysis of the fault gouge indicates the presence of extremely narrow clay zones (50–300 μm thick) that are interpreted as the fault rupture surfaces. Few shear indicators are observed outside of the fault gouge, implying that slip was localized within the gouge zone. Slip localization along a bed-parallel surface resulted in a narrow gouge zone that produced less high-frequency ground motion and larger displacements (average 8 m) during the earthquake than in the southern region. Displacement in the southern region averaged only 2 m, but ground shaking consisted of large amounts of high-frequency ground motion. The fault in the southern region dips 20°–30° at the surface and consists of a wide (20–70 m thick) zone of sheared, foliated shale with numerous gouge zones. These data demonstrate a potential correlation between fault structure (i.e., gouge width, geometry) and earthquake characteristics such as displacement and ground motion (i.e., acceleration).

Introduction

The M_w 7.6, 21 September 1999 Taiwan earthquake lasted 45 sec and ruptured along the Chelungpu fault in central Taiwan (Fig. 1). The earthquake produced steep, high (up to 12 m) fault scarps along an approximately 90-km-long, north–south trace. Earthquake damage, mostly the result of strong ground motion, caused over 2400 deaths (Shin and Teng, 2001). Ground acceleration increased from the south to the north along strike of the Chelungpu fault. The structure of the fault zone at different points along the fault, and its possible link to ground motion variability, is investigated in this article.

Seismic and rupture characteristics of the 1999 earthquake varied along strike. The change in rupture magnitude and ground motion along the fault trace has been well documented (Ma *et al.*, 2000, 2001; Chen *et al.*, 2001a; Dalguer *et al.*, 2001; Lin *et al.*, 2001). Slip and displacement increased toward the northern end of the rupture, while the greatest amounts of high-frequency ground acceleration occurred in the southern region near the epicenter. Rupture style changed from pure thrust near the epicenter (Dalguer *et al.*, 2001) to thrust displacement with a significant left-lateral component at the northern end of the fault trace (Chen *et al.*, 2001b; Lin *et al.*, 2001; CGS, 2002). Typical vertical displacements (heave) of 5–7 m in the northern region reached a maximum of 11.5 m at the Shihkang Dam on the Tachia River (Chen *et al.*, 2001a; Lee *et al.*, 2001b). Horizontal displacements (throw) in the northern region averaged 7–9 m and reached a maximum of 11.1 m (Chen *et al.*, 2001a; Lin *et al.*, 2001). Slip vectors were oriented 320°–330° based on surface rupture piercing points and Global Positioning System (GPS) data, indicating oblique thrust motion (Chen *et al.*, 2001a; Yu *et al.*, 2001). In contrast, the southern region had heave and throw displacements of approximately 2 m. Subsurface slip derived from inversion of strong motion data averaged 9 m with a maximum of 15 m in the northern region, while subsurface slip in the southern region was approximately 1–3 m (Ma *et al.*, 2001).

The dip of the fault also changes along strike. Dip mea-

*Present address: University of California, Santa Barbara, 1006 Webb Hall, Santa Barbara, California 93106; richard@crustal.ucsb.edu.

†Present address: Geology Department, Trinity College, Dublin, Ireland.

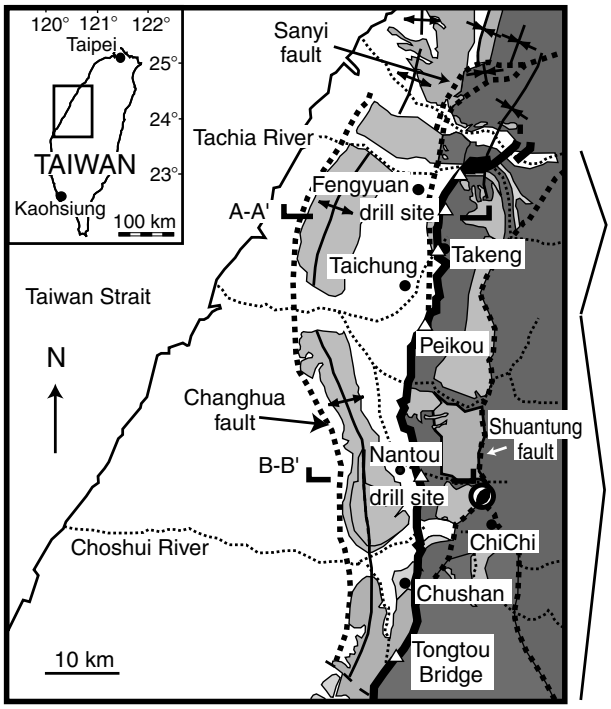

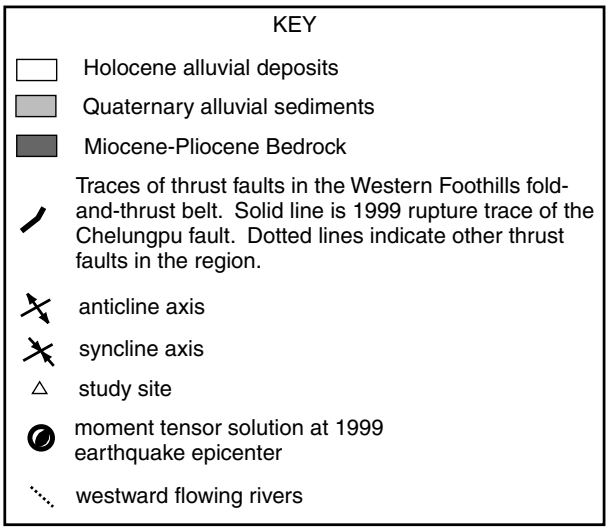

Figure 1. Generalized geologic map of the Chelungpu/Sanyi fault region, including the location of the Chelungpu fault trace. The regional location of geologic mapping is indicated on the Taiwan country map in the upper left corner of the figure. Cross sections AA′ and BB′ are indicated. All faults are east-dipping thrust faults. The epicenter location is from Shin and Teng (2001). Mapping is based on Chen *et al.* (2000), Hseih *et al.* (2001), and Chen *et al.* (2002).

surements from the fault scarp in the northern region were 50°–80° east (Lin *et al.*, 2001), in contrast to the 30°–35° dip measured from the scarp in the southern region (Lee *et al.*, 2001a). Focal mechanism solutions from the 1999 earthquake indicate that the fault ruptured along a 20°–30°, east-dipping fault between 5 and 10 km depth (Kao and Chen, 2000; Wang *et al.*, 2000; Ma *et al.*, 2001). Therefore, the fault can be considered a planar fault in the southern region but must bend or have a different geometry, at least near the surface, in the northern region.

Analysis of the fault zone was completed at three locations in the northern region and two locations in the southern region (Fig. 1). Structural data from the northern region were collected from a 450-m-long, 50°-inclined borehole to a true vertical depth (TVD) of 345 m through the fault just east of the city of Fengyuan (Fengyuan drill site) (Fig. 1). These data were combined with detailed analysis from a surface exposure of the fault in the Tali River, 6 km south of the drill site near the town of Takeng. The fault was also described at the fault scarp through the Tachia River, 5 km north of the Fengyuan drill site in the northern region (Fig. 1). Structural data from the southern region were collected from a vertical drillhole immediately southeast of Nantou City, as well as from a surface exposure of the fault at the southern terminus of the fault trace near the Tongtou Bridge along the Chingshui River (Fig. 1). Additionally, core data from two sites (Y. H. Lee, personal comm., 2002; Liao *et al.*, 2002), outcrop analysis (Lin *et al.*, 2001), and seismic reflection profiles (Chang, 1971; Wang *et al.*, 2000) are reviewed to examine the fault structure variations from the north to the south.

Drilling at Fengyuan and Nantou (Fig. 1) was completed from November 2000 through January 2001 as part of the Chelungpu Fault Drilling Project, funded by the Japanese Marine Science and Technology Center. Drilling into recently ruptured faults can reveal significant insight into their composition and structure (Ohtani *et al.*, 2000). The core not only provided samples of the fault zone at depth, but also allowed a determination of fault dip to a TVD of 250 m. Determination of fault dip is otherwise difficult due to the bed-parallel geometry of the fault, because seismic reflection shows bedding plane reflections similar to fault-plane reflections, making differentiation of a bed-parallel fault from bedding difficult. Our fault identification and dip determination through the drilled core thus provides a valuable data point for reconstructing the regional fault geometry in the near surface, which would otherwise be a difficult task.

Analysis of fault-zone structure may provide answers to the observed variation in the 1999 earthquake seismology. It is vital to determine whether slip is localized in a narrow zone or dispersed over a wide area. Why is the largest offset at the northern end of the rupture and not near the epicenter? What are the causes of the spatial variation in slip and surface displacement along strike? How does the geology within the upper few hundred meters of the surface affect fault rupture? Several models explain how energy is dissipated near the Earth's surface during an earthquake (Wald and Heaton, 1994; Brune and Anooshehpoor, 1998), but few data have been collected to determine which model best explains the distribution of slip along the fault. Models of fault dynamics (Kanamori and Heaton, 2000; Brodsky and Kanamori, 2001; Ma *et al.*, 2002) rely on understanding the thickness and roughness of fault surfaces. These models sug-

gest that the Chelungpu fault zone may act as a pressurized, viscous fluid. Additionally, models of the Chelungpu fault by Oglesby and Day (2001) and Oglesby *et al.* (2000) suggest that the near-surface fault dip affects the displacement and ground motion at the surface. By studying the near-surface structure of the active Chelungpu fault, we can examine fault width, dip, hanging-wall and footwall geology, and deformation traits of the fault zone along strike. These characteristics are then compared with observations of coseismic slip on the fault to determine a correlation between fault structure and rupture properties observed during the 1999 earthquake.

Geologic Setting

The Chelungpu fault is a west-vergent thrust fault along the boundary between the central mountains and the Taichung basin in central Taiwan (Fig. 1). It makes up the middle of three, north–south–trending thrust faults that form the active Western Foothills fold-and-thrust belt. The Chelungpu fault is structurally above the frontal thrust of the fold-and-thrust belt, the Changhua fault, which is located in the western coastal plain approximately 10 km west of the Chelungpu fault (Figs. 1, 2a). Thus, the recent earthquake was an out-of-sequence event within the fold-and-thrust belt (Morley, 1988; Kao and Chen, 2000; Wang *et al.*, 2000; Chen *et al.*, 2001b).

Tectonic shortening across Taiwan is driven by the Philippine Sea plate converging northwesterly with Eurasia at a relative rate of approximately 7 cm/yr (Seno *et al.*, 1993), accommodating at least 150 km of shortening (Suppe, 1980). The Chelungpu fault has accommodated an estimated 10–15 km of this shortening during the last ~1 Ma, based on balancing of regional cross sections (Suppe, 1980; Lee *et al.*, 2001a). Uplift in the Western Foothills region, associated with displacement on the Chelungpu fault, began approximately 1.25 Ma (Chen *et al.*, 2001) and places a maximum probable age on initiation of faulting. An approximate long-term slip rate of 10–15 mm/yr can be calculated for the Chelungpu fault from these data (Lee *et al.*, 2001a).

The northern region of the Chelungpu fault can be considered a bed-parallel thrust fault in the near surface. Near-surface fault outcrops define a steeply dipping (45°–80°) fault, parallel to bedding in the hanging wall and footwall, that ruptured with oblique left-lateral thrust motion (Chen *et al.*, 2001a; Lin *et al.*, 2001). The fault in the northern region is located within the hanging wall of the Old Chelungpu fault (Fig. 2a) along the western flank of the south-plunging Toukoshan syncline (Hung and Wiltschko, 1993; Lo *et al.*, 1999; Lee *et al.*, 2002). Outcrops of bedrock in the footwall and hanging wall expose 25°–70° east-dipping bedding of the Pliocene Chinsui Shale or the Miocene Kuechulin Formation. The footwall of the Chelungpu fault has up to 70 m of Quaternary alluvium overlying the bedrock. The alluvium depth is constrained with shallow (<100 m) drilling through the alluvium into Miocene–Pliocene bedrock (Y. H. Lee, personal comm., 2002). Further west, in the footwall of the Old Chelungpu fault, the Quaternary deposits are over 1500 m thick (Hung and Wiltschko, 1993). Therefore, the Old Chelungpu fault has a footwall ramp geometry, whereas the recent rupture on the active Chelungpu fault has a footwall flat geometry (Fig. 2a). The old Chelungpu fault trace is not preserved and is buried beneath Holocene alluvium and late Pleistocene terrace surfaces ~1 km west of the 1999 earthquake rupture (Fig. 1) (Ho and Chen, 2000).

The southern region of the Chelungpu fault differs from the northern region. The Pliocene Chinsui Shale and Miocene Kuechulin Formation in the hanging wall are juxtaposed with a thick sequence of Quaternary deposits across the fault (Fig. 2b). In this aspect the southern region is similar to the Old Chelungpu fault. Quaternary deposits in the footwall are relatively flat lying and are estimated between 2000 and 3000 m thick in the southern region (Chang, 1971; Lee *et al.*, 2001a). Miocene or Pliocene bedrock do not outcrop in the footwall, indicating the fault geometry is a footwall ramp. Bedding in the hanging wall in the southern region strikes 0° and dips 20°–40° east. Outcrops and seismic profiles in the southern region indicate the fault dips 20°–35° (Chang, 1971; Ho and Chen, 2000; Lee *et al.*, 2001a) east. Focal mechanism solutions from the 1999 earthquake indicate thrust motion that ruptured on a 15°–30°, east-dipping fault between 5 and 10 km depth (Hung and Suppe, 2000; Kao and Chen, 2000; Wang *et al.*, 2000; Ma *et al.*, 2001). The southern region therefore is a planar fault to depth (Fig. 2b). This southern region geometry contrasts with the northern region, where the steeply dipping (45°–80°) fault observed at the surface (Lin *et al.*, 2001; this work) implies that the fault bends in the subsurface from its gentler, 15°–30° dip (Fig. 2a).

Structural Data on the Fault

Northern Region

The fault structure in the northern region was analyzed in a 450-m-long core drilled through the fault (Fig. 3), at a fault exposure in the Tali River near the town of Takeng and at the fault scarp through the Tachia River (Fig. 1). Identification of the fault zone is based on a combination of gouge at the rupture surface, fracture density in the hanging wall, and displacement across the fault, although not all of these factors were used to characterize the fault at every location. For this analysis fractures are defined as any rupture, joint, break, or fault in the core that cuts through bedrock. The density of the fractures was determined quantitatively in the Fengyuan drill core and qualitatively from the other sites. Fault gouge is the zone of intense shearing and/or slip, usually associated with clay, intense foliation, and grain cataclasis. Gouge does not retain its original sedimentary structures and is easily distinguishable from the protolith.

The northern region of the Chelungpu fault is characterized by a narrow gouge zone located at the base of a zone

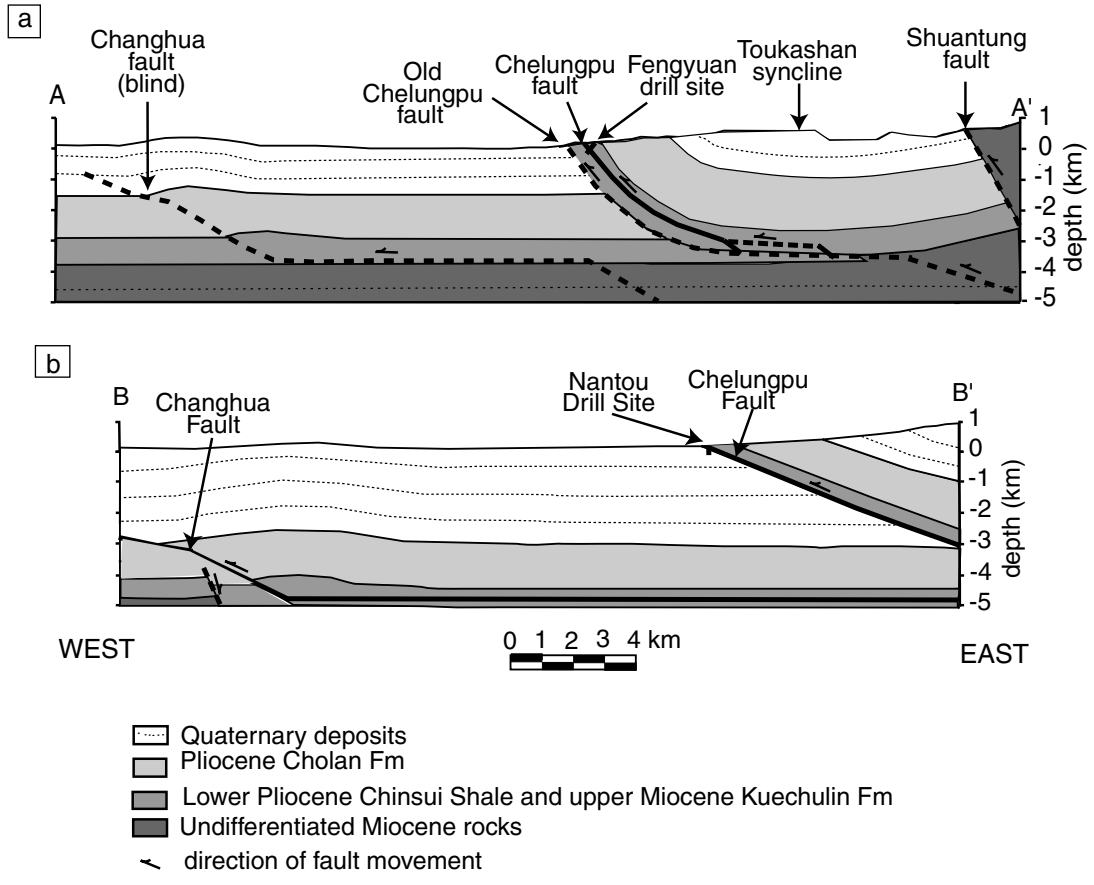

Figure 2. Cross sections (a) AA′ and (b) BB′ through the northern and southern regions of the Chelungpu fault. Faults are shown as bold black lines, which are dashed where approximated. The active rupture trace is shown in the hanging wall of the Old Chelungpu fault (a). Cross sections have no vertical exaggeration. Drillhole locations from Fengyuan (AA′) and Nantou City (BB′) are indicated. The subsurface geometry of the Chelungpu fault in AA′ is interpreted based geologic mapping (this study). Subsurface geometry of the Chelungpu fault in BB′ is based on seismic interpretation (Chang, 1971). Other geologic data used to complete the cross sections are from Ho and Chen (2000) and Lo and Wu (1999).

of increased fracture density. These properties are best observed in the Fengyuan drill core, which penetrated the fault at a depth of 250 m vertical depth. The fault dip was constrained at 53° east by aligning the surface trace with the fault surface in the core (Fig. 3). The primary rupture surface is interpreted based on the presence of fault gouge, striations, increased fracture density above the gouge, association with the largest fracture in the core, and location parallel to near-surface bedding. The fault gouge consists of a 7-mm, dark gray clay zone at the base of the largest (1.5 m wide) fracture (Fig. 4). An interesting feature of the fault is that fracture density increased asymmetrically 30–50 m above the fault in the hanging wall, but dropped off abruptly in the footwall (Fig. 5). Synthetic, smaller faults were observed above and below the primary Chelungpu fault (ruptured 21 September 1999) but do not have significant displacement relative to the primary fault. The Chelungpu fault is confined to bedding of the Kuechulin Formation, based on biostratigraphy (Huang *et al.*, 2002). No age determinations have been completed on the core, so the relative ages of the siltstone and shale across the fault are unknown, but there is nothing to suggest that the rocks are not in normal stratigraphic sequence across the fault. The surface rupture shows approximately 7–10 m of slip (J. C. Lee, personal comm., 2000), with Kuechulin Formation sandstone in both the hanging wall and footwall, consistent with a bed-parallel rupture. A more detailed description of the core and fracture density analysis may be found in Appendix A.

A surface outcrop of the Chelungpu fault was well exposed at a temporarily excavated locality 6 km south of the Fengyuan site near the town of Takeng in the Tali River (Figs. 1, 6). The fault juxtaposes siltstone (Miocene Kuechulin Formation or Pliocene Chinsui Shale) in the hanging wall with unconsolidated Quaternary fluvial gravel deposits in the footwall. These gravel deposits are approximately 70 m thick (Y. H. Lee, personal comm., 2002) and overlie silt-

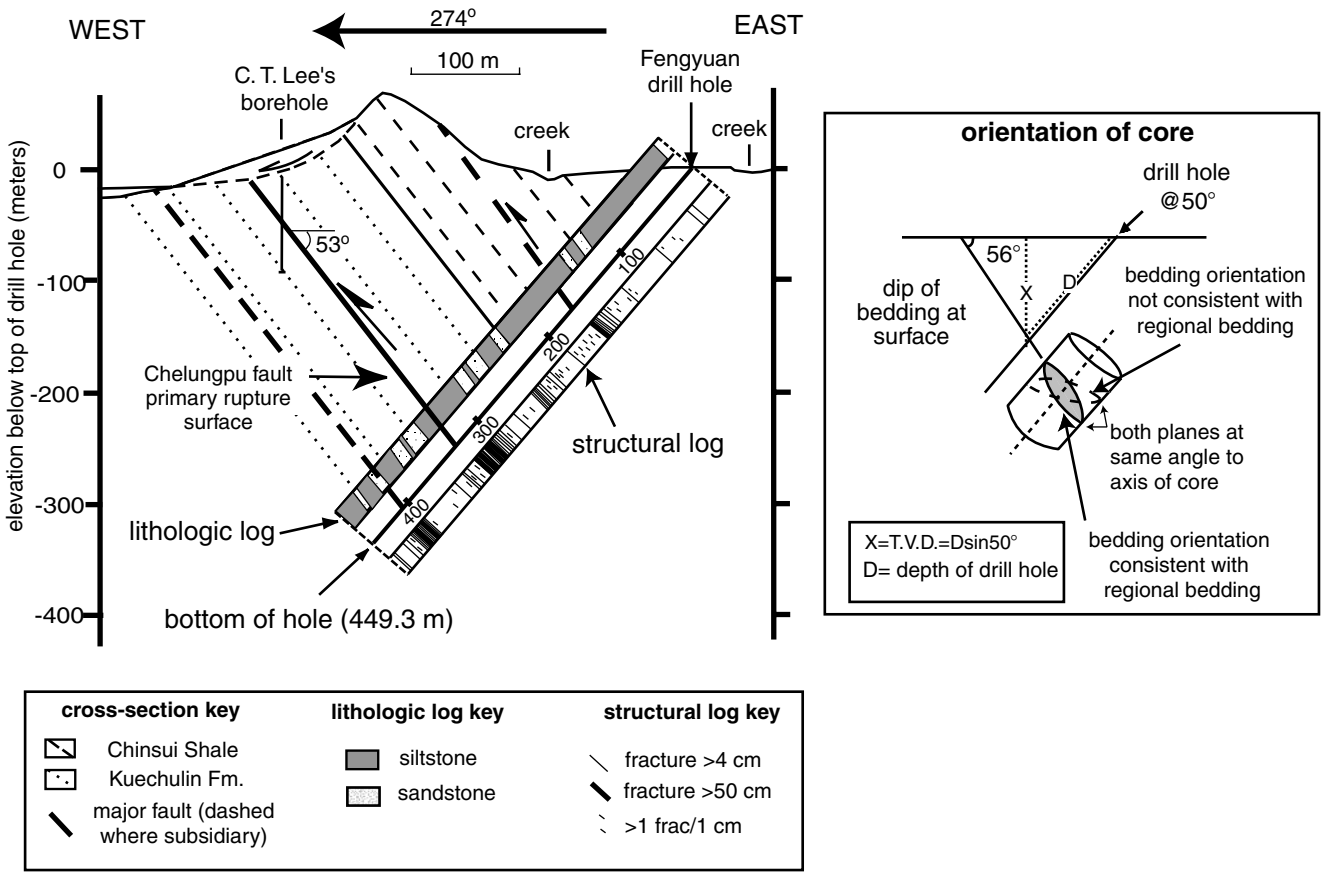

Figure 3. Cross section through the Fengyuan drill site (Fig. 12). The structural log indicates the location of fractures within the core. The largest fractures (>50 cm width) were extrapolated as bed-parallel subsidiary faults and are shown as bold dashed lines to the surface. The primary rupture surface of the Chelungpu fault was aligned with the surface trace determined from structural contours. The lithologic log shows the depth of siltstone and sandstone within the core at their appropriate dip determined from core and outcrop data. Contact between the Chinsui Shale and Kuechulin Formation is inferred at 225 m core depth based on an increase in the number of siltstone beds. The solid black line indicates the approximate formation boundary. The orientation of the core is shown in the sketch on the right. The bedding angle (<90°) was measured relative to the core axis. Because the strike of the bedding is known from surface outcrops, and drilling was perpendicular to regional bedding strike, the bedding measured in the core represented two possible dips at the surface. The correct dip (of the two possible dips) is determined (shaded ellipse) in the core by correlating with the surface outcrops. Surface geology is determined by detailed mapping around the drill site (this study).

stone similar to that in the hanging wall. This suggests that the fault plane is confined within the Miocene Kuechulin Formation and/or Pliocene Chinsui Shale to very near the surface, possibly along a bed-parallel, footwall-flat surface similar to that seen at the Fengyuan drill site. A distinctive, 20-cm-thick, dark gray clay gouge lies at the faulted siltstone/conglomerate contact (Fig. 6). Within 30 m of the gouge zone, intense fracturing of the siltstone makes bedding indistinguishable. This is interpreted to be similar to the zone of increased fracture density observed above the fault in the Fengyuan core. Beyond this zone, fracture density decreases and bedding is apparent. At least two synthetic faults with less than 1 m vertical displacement are apparent in the hanging wall, similar to synthetic faults observed in the Fengyuan core.

Microstructural and scanning electron microscopy analysis across the fault zone at the Takeng site reveals the deformation mechanisms and fabrics associated with the localized zone of slip. A complete description of these analyses can be found in Appendix B. Samples from the clay gouge at the fault contact reveal a foliated, clay-dominated fabric (Fig. 7d) in which dark zones less than 0.1 mm thick cut the clay fabric. Subparallel, parted surfaces are found only in the fault gouge zone and are interpreted as slip planes. The fractured siltstone protolith has not undergone bulk deformation, as evidenced by undeformed foramini-

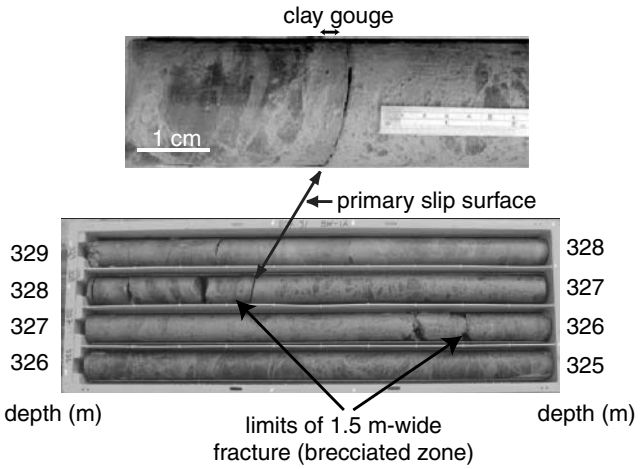

Figure 4. Photo of the Fengyuan core from 325 to 329 m. The close-up (upper photo) shows the primary slip surface of the 1999 rupture. The planar break through the middle of the upper photo is the surface that showed striations matching surface slip vectors. The break is associated with a thin, 7-mm, dark gray, planar, sheared clay gouge located at the base of a 1.5-m-wide fracture (brecciated zone).

ferid fragments centimeters from the slip surface (Fig. 7c). Backscattered scanning electron microscopic images of the fault surface (Fig. 8) reveal a zone 50–300 μm thick that is composed of disrupted and brecciated clay-rich gouge, which we interpret as the slip surface from the 1999 earthquake. These observations suggest that shear is localized in very narrow (50–300 μm) zones within the fault gouge.

The Chelungpu fault was observed at the Tachia River, 5 km north of the Fengyuan drill site, where the vertical offset on the fault created a 6-m-high waterfall through the river (Fig. 9). The Chinsui Shale is exposed in the hanging wall and strikes approximately 45°. The Kuechulin Formation is exposed near the fault trace in the footwall and parallels the hanging-wall bedding. Dips vary between 30° and 55° in the hanging wall and footwall. Bedding is very distinct and appears to be in stratigraphic sequence across the fault. Less than 1 m of alluvium covers the footwall bedrock in the river channel within 50 m of the fault. One 20-cm-wide brecciated zone was observed approximately 2 m from the rupture surface. Lee *et al.* (2002) documented three synthetic faults, parallel to bedding, in the hanging wall, but these faults showed cumulative vertical displacement of less than 1 m, which accounts for less than 10% of the total displacement during the earthquake. These are probably similar to the synthetic faults found at Fengyuan and Takeng. The fracture density in the hanging-wall and footwall bedrock is less than one fracture per 3 cm. The primary fault surface from the 1999 rupture was not observed as it was below the water level, but we suggest that slip localization occurred along a narrow fault based on the distinct scarp morphology across the river. The remarkably little deformation observed in the hanging wall of the fault, the intact stratigraphic sequence from the footwall into the hanging wall, and lack of footwall alluvium are evidence that this fault may be very young with little cumulative historic slip along a bed-parallel surface.

At all three northern-region localities the fault zone consists of a narrow (0.7–20 cm thick) gouge zone in the near surface (<250 m depth). The gouge is widest where it ruptured between siltstone and conglomerate in the uppermost 70 m at the Takeng site. The fault gouge is associated with an asymmetric zone of increased fracture density in the hanging wall. The fault ruptured parallel to both hanging-wall and footwall bedding.

Southern Region

Fault analysis in the southern region was completed on a drilled core through the fault near the town of Nantou, at the fault exposure at the Tongtou Bridge near the southern end of the fault trace, and in the Peikou Stream (Fig. 1). The southern region displays a much different structure from the northern region. A vertical hole was cored through the Chelungpu fault a few kilometers southeast of Nantou City as part of the Chelungpu fault drilling project (Fig. 1). The results from this drilling are published by Huang *et al.* (2002) and Tanaka *et al.* (2002), but qualitative analysis of this core is presented here. This hole penetrated the fault at approximately 180 m, indicating a fault dip of approximately 30° east, similar to the 35° dip measured in the southern region near Wufeng (Lee *et al.*, 2001a) (Fig. 1). The hanging wall consists of Pliocene Chinsui Shale, while the footwall consists of flat-lying Quaternary Toukoshan Formation conglomerate. The presence of a thick Quaternary package in the footwall implies a long history of displacement and a large cumulative slip on this fault.

The fault zone in the drill core is characterized by a 20-m-thick section of intensely foliated shale. This includes approximately 50% (10 m) of discontinuous brecciated zones and numerous fault gouge zones. Within 70 m of the contact, the bedrock was intensely deformed by foliation and fracturing. There was less than 15 m of "undeformed" (less than one fracture per 3 cm) Chinsui Shale in the 70 m above the fault. The fault zone in this drill core is clearly a diffuse zone, where shear has been distributed over a wide (>20 m) area.

The Tongtou Bridge over the Chingshui River is near the southern termination of the 1999 fault trace (Figs. 1, 10). Here the fault is interpreted to dip ~30° (Liu and Lee, 1998). Two meters of strike-slip and 0.4 m of vertical displacement occurred during the 1999 earthquake (Central Geological Survey of Taiwan [CGS] 1999). The footwall consists of relatively flat-lying Quaternary Toukoshan Formation. Near the fault, bedrock in the hanging wall consists of the Miocene Kuechulin Formation dipping 70°–80° southeast (Liu and Lee, 1998). This steep dip in the hanging wall only exists along the southernmost 5–10 km of the fault trace, from the point where the fault bends to the southeast just south of Chushan (Fig. 1). An ~60-m-wide region of intensely foliated shale with numerous (>20) gouge zones characterizes

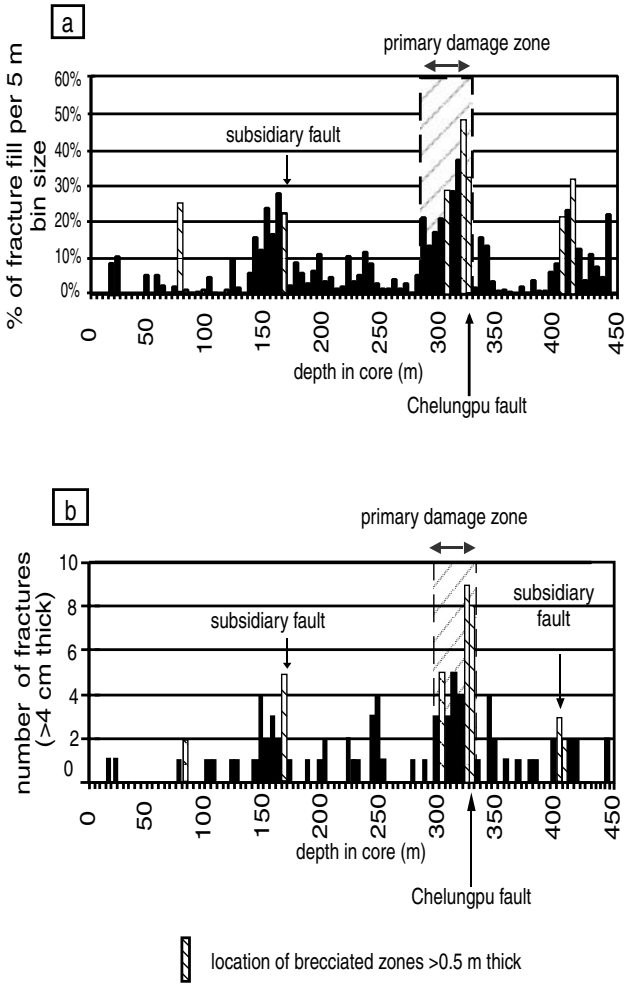

Figure 5. Histograms of fracture density in the core and their relation to the largest fractures. The location of the Chelungpu fault is indicated. (a) Method A showing the percentage of fracture fill per 5-m core length. (b) Method B showing the frequency of fractures greater than 4 cm thick within the core. Both histograms show an increase in fracture density at approximately 300 m core depth and an abrupt drop in fracture density below the Chelungpu fault rupture surface at 326 m. See Appendix A for a detailed description of the fracture analysis.

the fault in this region (Fig. 10). The gouge zones consist of sheared, foliated clay subparallel to bedding. The fault geometry is a footwall ramp, similar to the rest of the southern region.

Observations from other localities in the southern region are consistent with a wide, diffuse shear zone and gently dipping fault. Ho and Chen (2000) discussed outcrops at the Peikou Stream, where their observations indicate the fault zone consists of a 20-m-thick shear zone dipping 25° east. Drilling by the Central Geologic Survey through the Chelungpu fault zone to ~400 m depth in Chushan (Fig. 1) indicates that the fault dips 40° and is characterized by at least one 1-m-thick gouge zone within a wider "shear" zone (Y. H. Lee, personal comm., 2002).

Discussion

The 1999 rupture of the Chelungpu fault in Taiwan provides an ideal opportunity to study the structure of an active thrust fault, how this structure has evolved, and how the structure relates to coseismic displacement during a single earthquake event. Data collected in the northern region indicate that slip on the fault is confined to a narrow (0.7–20 cm) gouge zone. The gouge widens toward the free surface, and this could be due to the effect of change in lithology across the fault. Where the fault juxtaposes shale with unconslidated sedimentary units, the fault gouge becomes wider than where the fault is confined to a bed-parallel surface. At 250 m depth, where the shale is juxtaposed with shale, the fault is confined to a "smooth" shale bedding plane. The bed-parallel fault geometry in the north may have facilitated slip localization by orienting slip along existing planes of weakness (bedding). In contrast, the southern region fault geometry contains a footwall ramp juxtaposing Kuechulin Formation or Chinsui Shale with unconsolidated conglomerate for at least 2000 m down-dip in the near surface (Lee *et al.*, 2001a). Slip may have been inhibited along a "rough" zone between east-dipping Pliocene siltstone and shale and flat-lying Quaternary Toukoshan Formation, ultimately producing the wide shear zone.

Thrust faults near the surface can display either diffuse or localized fault zones (Carver and McCalpin, 1996). Diffuse fault zones normally do not produce steep fault scarps and generally form gentle, up-warped scarp surfaces, sometimes manifested in fault-related folding. Fault-related folding was documented near Wufeng in the southern region, where the fault is a diffuse zone (Lee *et al.*, 2001a). The northern region of the Chelungpu fault behaves as a localized zone with a single, large-displacement surface offset and a discrete fault plane beneath the surface, as evidenced by the core logging and outcrop mapping.

The dip of the Chelungpu fault to 250 m TVD was determined by aligning the surface trace with fault gouge in the core. The dip of approximately 53° correlates well with the dip measured on the fault at Takeng (48°) and bedding in the hanging wall (average 56° ± 20°) and footwall (average 53° ± 4°) near the Fengyuan drill site (Appendix A). Measurements of the scarp near the drill site indicate a near-surface fault dip of 50°–80° (Lin *et al.*, 2001). Additional constraints on the fault dip are provided by data collected from an ~100-m-deep borehole (BH-2) approximately 0.5 km northwest of the Fengyuan drill site. BH-2 was drilled by C. T. Lee from National Central University in Taiwan and showed that the fault has a dip of approximately 60° (Fig. 3) (C. T. Lee, personal comm., 2002). Interestingly, focal mechanisms for the mainshock and immediate aftershocks of the 1999 earthquake constrain the fault dip between 25° and 30° east at 5–10 km depth (Fig. 2) (Hung and Suppe, 2000; Kao and Chen, 2000; Wang *et al.*, 2000; Ma *et al.*, 2001; Shin and Teng, 2001; Lee *et al.*, 2002). This indicates there must be a bend in the fault in the northern

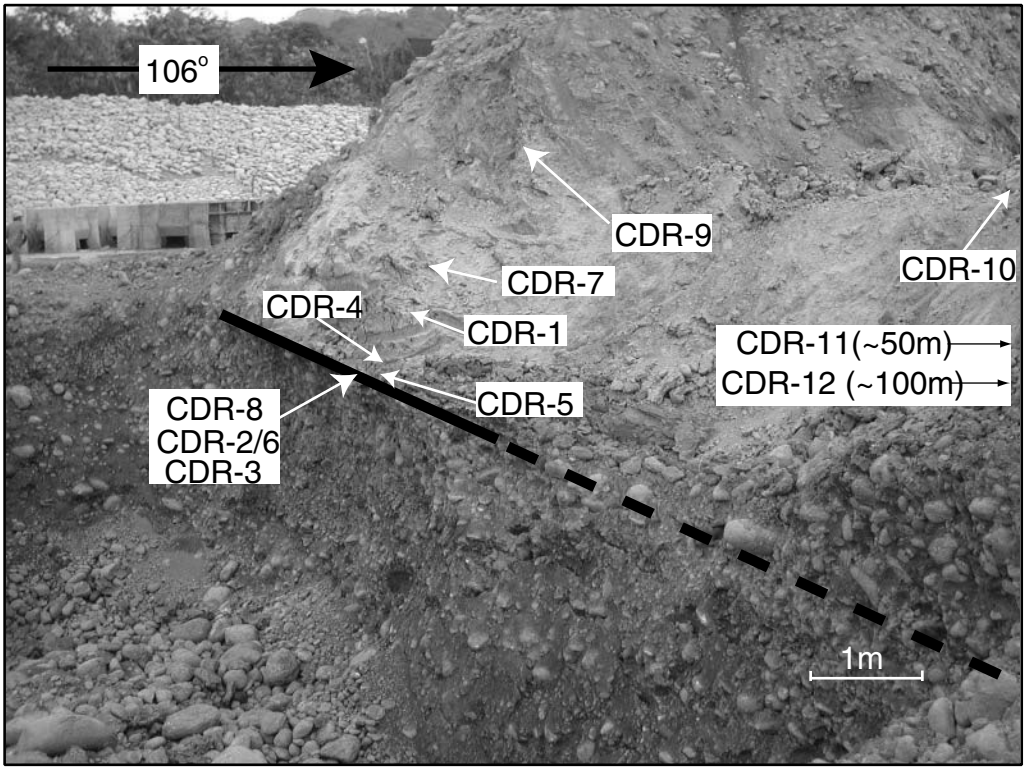

Figure 6. Oblique photo of the Chelungpu fault in the Tali River, near Takeng. The fault strikes 300° and dips 48° east. Pliocene or Miocene siltstone and mudstone (probably Chinsui Shale or Kuechulin Formation) is placed over Quaternary alluvial deposits. Sample locations are indicated. Siltstone within 20 m of the fault is intensely fractured and determined to be the damage zone related to the primary rupture trace. The fault gouge is 20 cm thick and is at the location of the thick black line on the photo, which is dashed where inferred.

region. Dips measured on the Chelungpu fault in the southern region correspond with the moment tensor solutions from depth, indicating that the fault is likely planar there (Lee *et al.*, 2001a). These regions of changing geometry match the regions of different rupture characteristics, indicating a possible relationship between fault geometry, slip zone composition, and fault rupture properties.

Brecciated Zone Formation

The origin of the damage zone asymmetry is uncertain. GPS data indicate that 90% of the coseismic movement during the earthquake occurred in the hanging wall (Lin *et al.*, 2001; Yu *et al.*, 2001), implying that the footwall was nearly fixed in an absolute reference frame on the timescale of an individual earthquake. Brune (2001) provided evidence for similar asymmetry of damage in thrust faults in southern California resulting from larger ground motion in the hanging wall than in the footwall. The damage zone deformation could therefore be mainly coseismic or perhaps aftershock related.

Alternatively, the damage zone could be an inherited aspect of the fault zone, formed deeper in the crust where the hanging wall was deformed as it moved from a flat to a ramp. At a flat-ramp "corner," there would be localized shortening in the hanging wall. Shortening could potentially deform the hanging-wall rocks at such corners. These zones would be subsequently carried up by the fault in the hanging wall over time, resulting in an asymmetric damage zone.

A third alternative is that the brecciated zones form "passively" from fluid flow in areas of increased fracture density. Fluid flow through fractures causes disintegration of the host rock around the fractures. This would widen the fractures, until the widening fracture network isolates clasts of the protolith (Regenfuss *et al.*, 1999). These clasts "fall" into the fracture that is filled with a matrix composed of the disintegrating protolith rock. This hypothesis works well for the brecciated zones in the Chelungpu fault. Fracture density is increased near the fault, and the muddy matrix in the zones is compositionally indistinct from the protolith. There is likely to have been fluid flow through the fractures of the fault zone in the near surface, based on high pore pressure observed in industry drillholes (Suppe, 1987) and well-sorted sedimentary formations in the area. But there is little evidence for shearing in the brecciated zones. These characteristics would support a "passive" method of brecciated zone formation.

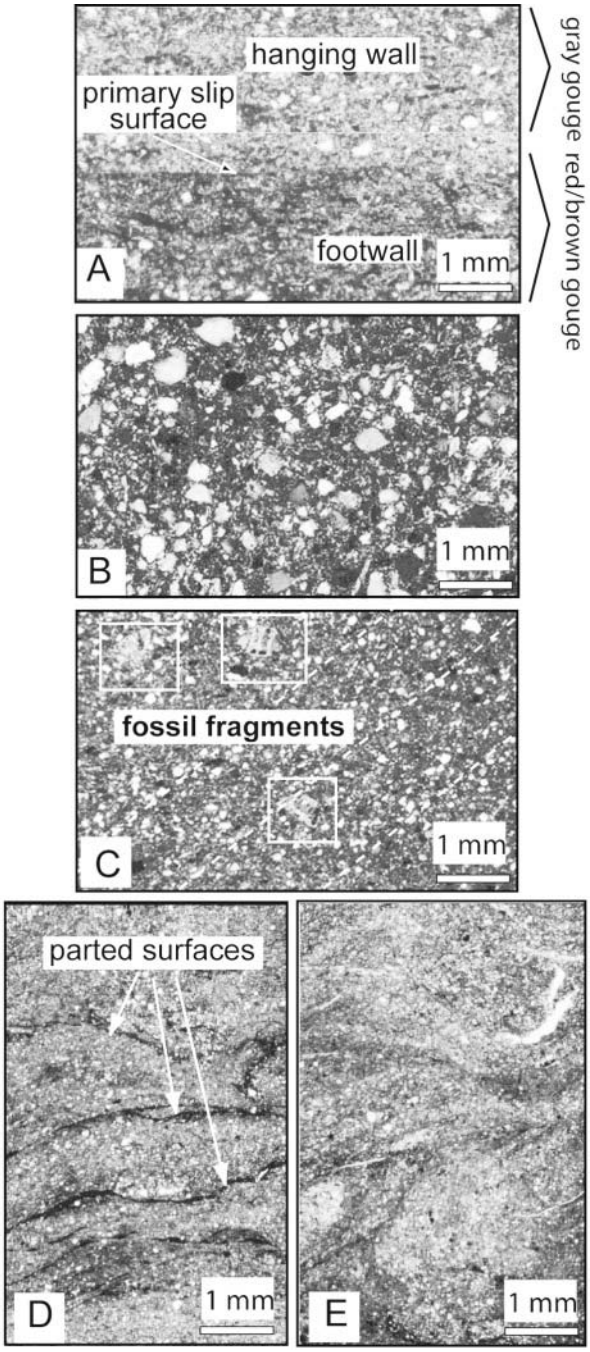

Figure 7. Cross-polarized photomicrographs from the 1999 rupture surface of the Chelungpu fault and hanging-wall rocks from the Tali River outcrop. Sample locations are shown in Figure 6. (a) The 1999 rupture surface, CDR-8, with hanging-wall siltstone and footwall Holocene alluvial deposit. The trace of the 1999 rupture is a 1- to 2-mm-thick horizon in the center of the photo. (b) Protolith sample CDR-11, 55 m northeast of the slip surface, shows texturally mature Pliocene siltstone with no evidence of deformation. (c) Hanging-wall sample CDR-5, from 20 cm above the slip surface, within the protolith, exhibits a faint foliation (white dashed lines) and undeformed foraminiferid fragments (white boxes). (d) Sample CDR-2/6, 5 cm above slip surface, within the fault gouge, with narrow faults marked by very fine grained dark horizons (parted surfaces). (e) Foliated fabrics from sample CDR-8 of clay gouge adjacent to the slip surface. Refer to the text for the description of textures.

Rupture Properties

The observations of high displacement and relatively low frequency ground motion along the northern region of the Chelungpu fault may be explained by fault structure. Fault zones may exhibit variations in thickness and slip distribution along strike and down-dip (Evans, 1990; Imber *et al.*, 2001). Observations made from the Fengyuan core combined with surface observations from Takeng suggest that slip is localized on a narrow gouge zone to depths of at least 250 m. We suggest that extreme slip localization in the near surface reflects the presence of a narrow slip surface at depth and that the fault is parallel to and guided by bedding. The presence of this very narrow (50–300 μm), clay-rich slip surface supports fault models (Kanamori and Heaton, 2000; Brodsky and Kanamori, 2001) in which narrow, lubricated fault zones can have reduced coefficients of dynamic friction during faulting. Surface displacements almost equal the displacements inverted from the seismic models (Chen *et al.*, 2001a; Lin *et al.*, 2001; Ma *et al.*, 2001), implying that all of the coseismic slip was confined to the narrow gouge zone along the fault scarps. Narrow slip surfaces have been documented along exhumed strike-slip fault zones (Chester and Chester, 1998), on *in situ* faults that slipped seismically (Gay and Ortlepp, 1979), and in other large-displacement thrusts (Gretener, 1972, 1977; Brock and Engelder, 1977; Price, 1988). These observations and those described in this article indicate that the extremely narrow, "knife-edge" nature of these faults may extend from the surface to considerable depth. These surfaces could either form early in the growth of a fault system and accommodate much of the subsequent slip in a fault zone (Shipton and Cowie, 2001) or they may be the result of slip localization after the formation of the damaged zone (Brock and Engelder, 1977). Narrow slip zones are also consistent with thermodynamic models of coseismic faulting events (Kanamori and Heaton, 2000; Brodsky and Kanamori, 2001). This investigation demonstrates an association between a narrow, localized slip surface with a large-displacement surface rupture. Slip constrained to such narrow slip planes may have reduced high-frequency energy radiation (>1 Hz) during a large-magnitude earthquake, as occurred during the 1999 event (Ma *et al.*, 2002).

The narrow zone that we interpret as the principal slip surface at the northern end of the fault has implications for the energetics of faulting. Sibson (1973) and McKenzie and Brune (1972) have shown that dry frictional slip of 1–10 m should produce temperatures high enough to melt the fault rocks, and yet this is rarely observed (Sibson, 1973). Rocks in the two cores drilled through the tip region of the Chelungpu fault are clearly deformed, but there are remarkably few veins of any type and no injection structures associated with the main slip surface.

Sibson (1973) pointed out that lack of melt in faults constrains the conditions under which the fault slips. The temperatures can be reduced if (1) the frictional strength of the fault is low or (b) there are pore fluids present, which

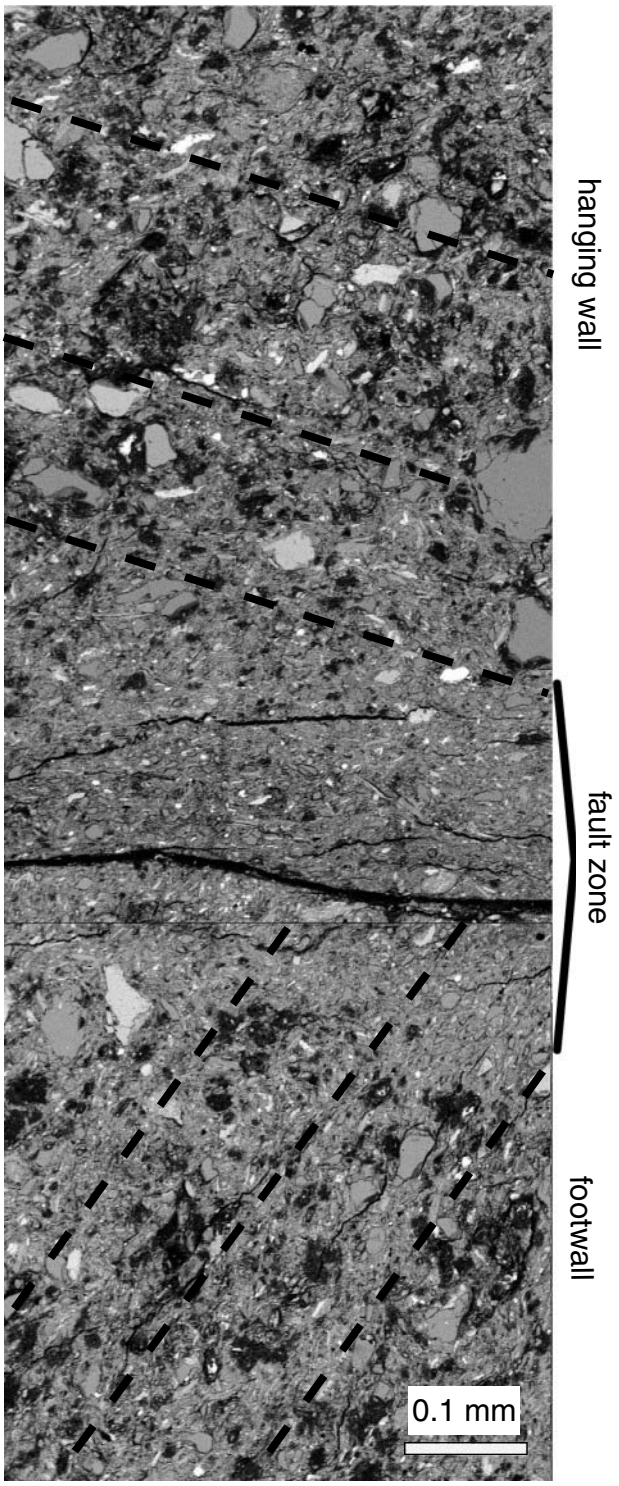

Figure 8. Scanning electron microscope image of the Chelungpu fault slip surface from sample CDR-8. Intra- and intergranular fractures and a random fabric characterize the fault zone, whereas rocks in the hanging wall and footwall have a well-defined clay-rich foliation (dashed black lines). The sense of shear is unknown, but is probably oblique with hanging wall to the left. The thin black zone near the center of the image is a small gap along the interpreted slip surface.

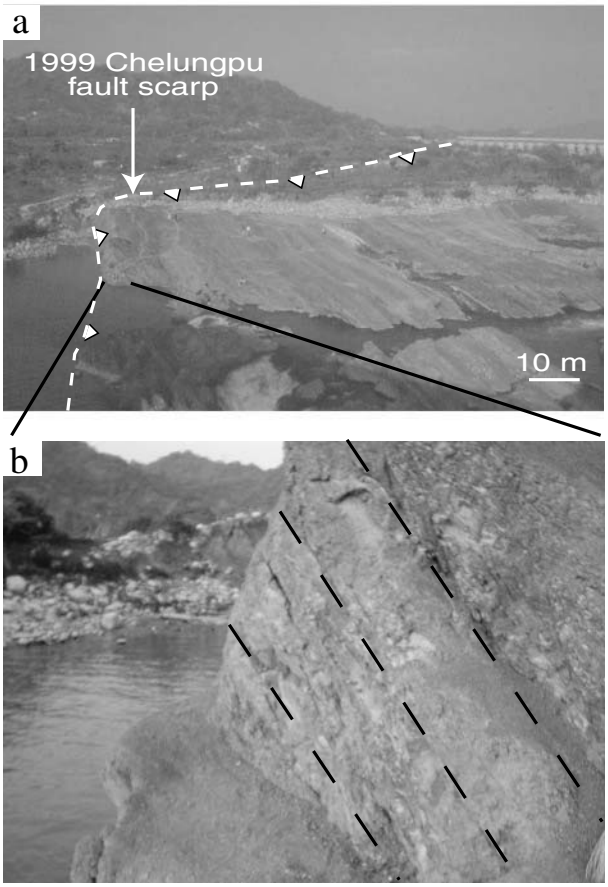

Figure 9. Chelungpu fault scarp at the Tachia River (Fig. 1). (a) Fault trace through the Tachia River indicated by a white, dashed line. Teeth are on hanging wall (up-thrown) side of the scarp. The total displacement on the fault at this location during the earthquake is approximately 10 m. The view is to the northeast. (b) Close-up view approximately 2 m above the fault surface in the hanging wall. The field of view is approximately 3 m vertical. The bedding of the Chinsui Shale is well preserved and dips toward the southeast (black dashed lines).

increase the fault's ability to adsorb heat and decrease normal stress on the fault. Recent work on slip on thin fault surfaces (Brodsky and Kanamori, 2001), considerations of a thermally induced pulse of water (Andrews, 2002), slip by a constrained wrinkle-like pulse along the fault (Andrews and Ben-Zion, 1997), or acoustic fluidization (Melosh, 1996) all require, or the effects are enhanced by, slip being restricted to a narrow surface in the absence of melting. Thus, while our data are from shallow levels, they support mechanisms in which slip is constrained to a narrow zone, with little or no off-fault dilation to arrest rupture.

Lithology variation along strike may have also contributed to the observed large displacement and strong ground motion variations along the Chelungpu fault. Displacement in the northern region along a bedding plane between similar siltstone or shale lithologies would act as a relatively low

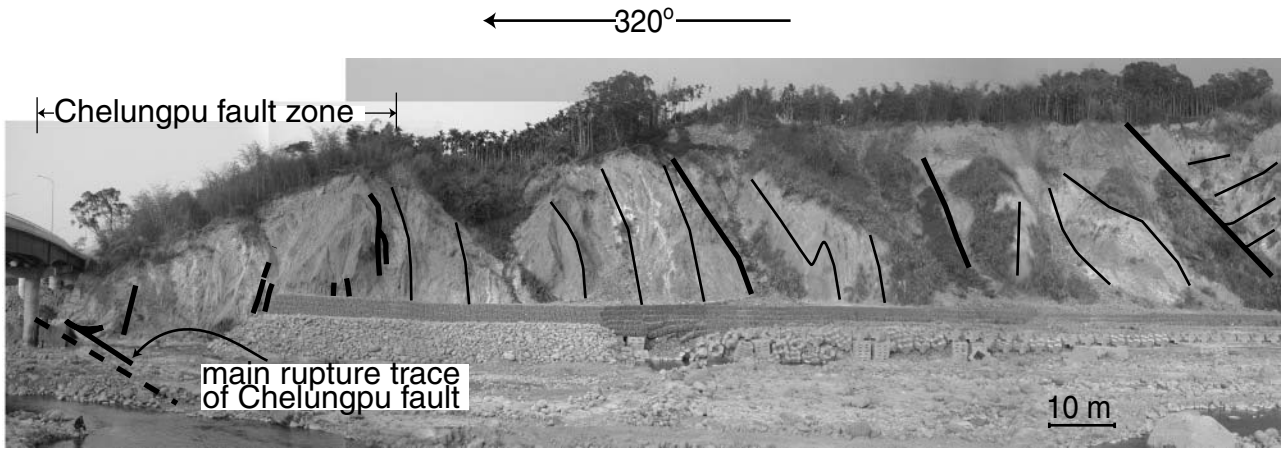

Figure 10. Oblique view of Chelungpu fault outcrop in the Chingshui River near the Tongtou Bridge. The Chelungpu fault is the thick dashed line beneath the Tungtou Bridge on the left of the photo. Bold black lines indicate fault gouge zones that are 10–50 cm thick. The fault zone consists of foliated shale and many gouge zones. Bedding is indistinguishable in the Chelungpu fault zone. Outside of the fault zone bedding dips are shown as thin black lines. Bedding in the hanging wall of the fault consists of the Kuechulin Formation (Liu and Lee, 1998), generally dipping steeply southeast but folded in places. The photo was taken facing northeast.

friction surface for slip. The result may be a smooth, low-frequency rupture with large displacement. In contrast, displacement between flat-lying conglomerate and 30°-dipping siltstone in a relatively wide gouge zone might be a relatively high friction zone, resulting in less displacement but higher frequency ground motion.

Factors such as fault width and ramp-flat geometry are readily identifiable prior to rupture. Our hypothesis that a narrow fault zone along a smooth surface (bedding plane) will produce lower frequency ground motion but possibly higher slip amounts than a wider fault zone along a rough surface (i.e., conglomerate/sandstone contact) can be easily tested with past and future earthquake rupture data. Our data clearly show a relationship between fault width, surface displacement, and ground motion on the Chelungpu fault, Taiwan, but data from other ruptures will either support or refute this hypothesis.

Conclusions

By combining core logging, structural analysis, and field mapping, we have identified the different structures of the northern and southern regions of the Chelungpu fault. The northern region of the Chelungpu fault dips ~52° to at least 250 m and has a flat-on-flat geometry. The bed-parallel geometry has resulted in a narrow fault gouge where slip is localized in 50- to 300-μm-thick zones. The fault zone in the southern region consists of a 20-m-wide diffuse zone of shearing that produced less surface displacement but more high-frequency ground motion. High-frequency ground accelerations were 50%–70% lower in the northern region than near the epicenter, but surface displacement was 200%–300% greater (Lin *et al.*, 2001; Ma *et al.*, 2001). The data presented in this article suggest that the existence of a narrow slip surface causes slip localization, large displacements, and less high-frequency ground motion during an earthquake. If our correlation is correct, then the fault width could control the coseismic rupture characteristics during an earthquake, specifically for thrust faults. The implication of these findings is that ground-motion predictions may be accurately determined based on *in situ* fault properties. The data collected on the structure and rupture characteristics from the active Chelungpu thrust fault provide insight into fault processes that can be applied to studies from older, exhumed thrust faults, as well as help us understand the characteristics of active faulting and future earthquakes.

Acknowledgments

Funding for this work came from National Science Foundation Grant EAR-0098108. The Japanese Marine Science and Technology Center and National Central University in Chungli, Taiwan, helped to support the drilling. We thank *Bulletin* reviewers Rick Sibson and two anonymous reviewers for their comments on an earlier version of this article. Thanks to M. Ando, H. Tanaka, A. Sakaguchi, J. H. Hung, J. C. Lee, Y. H. Lee, C. T. Lee, C. T. Wang, and other collaborators in both Japan and Taiwan.

References

Andrews, D. J., and Y. Ben-Zion (1997). Wrinkle-like slip pulse on a fault between different materials, *J. Geophys. Res.* **102,** 552–571.

Bekins, B., A. M. McCaffrey, and S. J. Dreiss (1994). Influence of kinetics on the smectite to illite transition in the Barbados accretionary prism, *J. Geophys. Res.* **99,** 18,147–18,158.

Brock, W. G., and T. Engelder (1977). Deformation associated with the movement of the Muddy Mountain overthrust in the Buffington window, southeastern Nevada, *Geol. Soc. Am. Bull.* **88,** 1667–1677.

Brodsky, E. E., and H. Kanamori (2001). Elastohydrodynamic lubrication of faults, *J. Geophys. Res.* **106,** 16,357–16,374.

Brune, J. N. (2001). Shattered rock and precarious rock evidence for strong asymmetry in ground motions during thrust faulting, *Bull. Seism. Soc. Am.* **91,** 441–447.

Brune, J. N., and A. Anooshehpoor (1998). A physical model of the effect of a shallow weak layer on strong ground motion for strike-slip ruptures, *Bull. Seism. Soc. Am.* **88,** 1070–1078.

Caine, J. S., J. P. Evans, and C. B. Forster (1996). Fault zone architecture and permeability structure, *Geology* **24,** 1025–1028.

Carver, G. A., and J. P. McCalpin (1996). Paleoseismology of compressional and tectonic environments, in *Paleoseismology*, J. P. McCalpin (Editor), Academic, New York, 183–270.

Central Geological Survey of Taiwan (CGS) (1999). Surface ruptures along the Chelungpu fault during the Chi-Chi earthquake (map), scale 1:25,000.

Central Geological Survey of Taiwan (CGS) (2002). Ground ruptures of the September 21, 1999 Chi-Chi earthquake (II), Ministry of Economic Affairs, Taipei, R.O.C., scale 1:50,000.

Chang, H. C. (1994). The geological map and explanatory text of Tachia, Taiwan, Central Geologic Survey, Ministry of Economic Affairs, R.O.C., scale 1:50,000.

Chang, S. L. (1971). Subsurface geologic study of the Taichung Basin, Taiwan, *Petrol. Geol. Taiwan* **8,** 21–45.

Chen, C. H., H. C. Ho, K. S. Shea, W. Lo, W. H. Lin, H. C. Chang, C. S. Huang, C. W. Lin, G. H. Chen, C. N. Yang, and Y. H. Lee (2000). Geologic map of Taiwan, Central Geologic Survey, Ministry of Economic Affairs, R.O.C., scale 1:500,000.

Chen, W. S., B. S. Huang, Y. G. Chen, Y. H. Lee, C. N. Yang, C. H. Lo, H. C. Chang, Q. C. Sung, N. W. Huang, C. C. Lin, S. H. Sung, and K. J. Lee (2001a). 1999 Chi-Chi earthquake: a case study on the role of thrust-ramp structures for generating earthquakes, *Bull. Seism. Soc. Am.* **91,** 986–994.

Chen, Y. G., W. S. Chen, J. C. Lee, Y. H. Lee, C. T. Lee, H. C. Chang, and C. H. Lo (2001b). Surface rupture of 1999 Chi-Chi earthquake yields insights on active tectonics of central Taiwan, *Bull. Seism. Soc. Am.* **91,** 977–985.

Chen, Y. G., W. S. Chen, Y. Wang, P. W. Lo, T. K. Liu, and J. C. Lee (2002). Geomorphic evidence for prior earthquakes: lessons from the 1999 Chi-Chi earthquake in central Taiwan, *Geology* **30,** 171–174.

Chester, F. M., and J. S. Chester (1998). Ultracataclasite structure and friction processes of the Punchbowl fault, San Andreas system, California, *Tectonophysics* **295,** 199–221.

Chester, F. M., and J. M. Logan (1986). Implications for mechanical properties of brittle faults from observations of the Punchbowl fault zone, California, *Pure Appl. Geophys.* **124,** 79–106.

Covey, M. (1984). Lithofacies analysis and basin reconstruction, Plio-Pleistocene western Taiwan foredeep, *Petrol. Geol. Taiwan* **20,** 53–83.

Dalguer, L. A., J. D. Irikura, J. D. Riera, and H. C. Chiu (2001). The importance of the dynamic source effects on strong ground motion during the 1999 Chi-Chi, Taiwan, earthquake: brief interpretation of the damage distribution on buildings, *Bull. Seism. Soc. Am.* **91,** 1112–1127.

Evans, J. P. (1990). Thickness-displacement relationships for fault zones, *J. Struct. Geol.* **12,** 1061–1066.

Gay, N. C., and W. D. Ortlepp (1979). Anatomy of a mining-induced fault zone, *Geol. Soc. Am. Bull.* **90,** 47–58.

Gretener, P. E. (1972). Thoughts on overthrust faulting in a layered sequence, *Bull. Can. Petrol. Geol.* **20,** 583–607.

Gretener, P. E. (1977). On the character of thrust faults with particular reference to the basal tongues, *Bull. Can. Petrol. Geol.* **25,** 110–122.

Ho, H. C., and M. M. Chen (2000). The geologic map and explanatory text of Taichung, Taiwan, sheet 24, Central Geologic Survey, Ministry of Economic Affairs, R.O.C., scale 1:50,000.

Hsieh, M. L., Y. H. Lee, T. S. Shih, S. T. Lu, and W. Y. Wu (2001). Could we have prelocated the northeastern portion of the 1999 Chi-Chi earthquake rupture using geological and geomorphic data? *Terr. Atmos. Ocean. Sci.* **12,** 461–484.

Huang, S.-T., J.-C. Wu, J.-H. Hung, and H. Tanaka (2002). Studies of sedimentary facies, stratigraphy, and deformation structures of the Chelungpu fault zone on cores from drilled wells in Fengyuan and Nantou, central Taiwan, *Terr. Atmospher. Ocean Sci.* **113,** 253–278.

Hung, J. H., and J. Suppe (2000). Subsurface geometry of the Chelungpu fault and surface deformation style, *Int. Workshop Annual Commem. Chi-Chi Earthquake* **1,** 133–144.

Hung, J. H., and D. V. Wiltschko (1993). Structure and kinematics of arcuate thrust faults in the Miaoli-Cholan area of western Taiwan, *Petrol. Geol. Taiwan* **28,** 59–96.

Imber J., R. E. Holdsworth, C. A. Butler, and R. A. Strachan (2001). A reappraisal of the Sibson-Scholz fault zone model: the nature of the frictional to viscous ("brittle-ductile") transition along a long-lived, crustal-scale fault, Outer Hebrides, Scotland, *Tectonics* **20,** 601–624.

Kanamori, H., and T. H. Heaton (2000). Microscopic and macroscopic physics of earthquakes, in *Geocomplexity and the Physics of Earthquakes*, American Geophysical Monograph **120,** 147–161.

Kao, H., and W. P. Chen (2000). The Chi-Chi earthquake sequence: active, out-of-sequence thrust faulting in Taiwan, *Science* **288,** 2346–2349.

Lee, J. C., H. T. Chu, J. Angelier, Y. C. Chan, J. C. Hu, C. Y. Lu, and R. ? J. Rau (2002). Geometry and structure of northern surface ruptures of the 1999 M_w = 7.6 Chi-Chi, Taiwan earthquake: influence from inherited fold belt structures, *J. Struct. Geol.* **24,** 173–192.

Lee, J. C., Y. G. Chen, K. Sieh, K. Mueller, W. S. Chen, H. T. Chu, Y. C. Chan, C. R. Rubin, and R. Yeats (2001a). A vertical exposure of the 1999 surface rupture of the Chelungpu fault at Wufeng, western Taiwan: structural and paleoseismic implications for an active thrust fault, *Bull. Seism. Soc. Am.* **91,** 914–929.

Lee, Y. H., W. Y. Wu, T. S. Shih, S. T. Lu, M. L. Shieh, and H. C. Cheng (2001b). Deformation characteristics of surface ruptures of the Chi-Chi earthquake, east of the Pifeng bridge, *Central Geol. Surv. Spec. Issue* **12,** 27–40 (in Chinese).

Liao, C. F., J. H. Hung, and C. T. Lee (2002). Analysis of clay minerals and fractures from cores of Chelungpu fault zone (abstract), in *Geologic Society of China, Annual Meeting*, *Abstracts with Programs*, 21–22 March 2002, 25–26.

Lin, A., T. Ouchi, A. Chen, and T. Maruyama (2001). Co-seismic displacements, folding and shortening structures along the Chelungpu surface rupture zone occurred during the 1999 Chi-Chi (Taiwan) earthquake, *Tectonophysics* **330,** 225–244.

Liu, H. C., and J. F. Lee (1998). The geological map and explanatory text of Yun Lin, Taiwan, Central Geologic Survey, Ministry of Economic Affairs, R.O.C., scale 1:50,000.

Lo, W., L. C. Wu, and H. W. Chen (1999). The geological map and explanatory text of Kuohsing, Taiwan, Central Geologic Survey, Ministry of Economic Affairs, R.O.C., scale 1:50,000.

Ma, K. F., E. E. Brodsky, J. Mori, C. Ji, T. R. A. Song, and H. Kanamori (2002). Evidence for fault lubrication during the 1999 Chi-Chi, Taiwan, earthquake (M_w 7.6) *Geophys. Res. Lett.* **30,** 48-1–48-4.

Ma, K. F., J. Mori, S. J. Lee, and S. B. Yu (2001). Spatial and temporal distribution of slip for the the 1999 Chi-Chi, Taiwan, earthquake, *Bull. Seism. Soc. Am.* **91,** 1069–1087.

Ma, K. F., T. R. A. Song, S. J. Lee, and H. I. Wu (2000). Spatial slip distribution of the September 20, 1999, Chi-Chi, Taiwan, earthquake (M_w 7.6): inverted from teleseismic data, *Geophys. Res. Lett.* **27,** 3417–3420.

McKenzie, D., and J. N. Brune (1972). Melting on fault planes during large earthquakes, *Geophys. J. R. Astr. Soc.* **29,** 65–68.

Melosh, H. J. (1996). Dynamical weakening of faults by acoustic fluidization, *Nature* **379,** 601–606.

Morley, C. K. (1988). Out of sequence thrusts, *Tectonics* **7,** 539–561.

Oglesby, D. D., R. J. Archuleta, and S. B. Nielson (2000). The three-dimensional dynamics of dipping faults, *Bull. Seism. Soc. Am.* **90,** 616–628.

Oglesby, D. D., and S. M. Day (2001). The effect of fault geometry on the 1999 Chi-Chi (Taiwan) earthquake, *Geophys. Res. Lett.* **28,** 1831–1834.

Ohtani, T., K. Fujimoto, H. Ito, H. Tanaka, N. Tomida, and T. Higuchi (2000). Fault rocks and paleo-to-recent fluid characteristics from the borehole survey of the Nojima fault ruptured in the 1995 Kobe earthquake, Japan, *J. Geophys. Res.* **105,** 16,161–16,172.

Price, R. A. (1988). The mechanical paradox of large overthrusts, *Geol. Soc. Am. Bull.* **100,** 1898–1908.

Regenfuss, S. M., J. M. Strickland, and J. D. Cooper (1999). Late Ordovician breccias in a Middle Ordovician orthoquartzite, southern Great Basin: evidence for unusual paleokarst (abstracts with programs), *Geol. Soc. Amer.* **31,** 99.

Seno, T., S. Stein, and A. Gripp (1993). A model for the motion of the Philippine sea plate consistent with NUVEL-1 and geological data, *J. Geophys. Res.* **98,** 17,941–17,948.

Shin, T. C., and T. Teng (2001). An overview of the 1999 Chi-Chi earthquake, *Bull. Seism. Soc. Am.* **91,** 895–913.

Shipton, Z. K., and P. A. Cowie (2001). Damage zone and slip-surface evolution over μm to km scales in high-porosity Navajo sandstone, Utah, *J. Struct. Geol.* **23,** 1825–1844.

Sibson, R. H. (1973). Interactions between temperature and pore-fluid pressure during earthquake faulting and a mechanism for partial or total stress relief, *Nature* **243,** 66–68.

Suppe, J. (1980). A retrodeformable cross section of northern Taiwan, *Proc. Geol. Soc. China* **23,** 46–55.

Suppe, J. (1987). The active Taiwan Mountain Belt, in *The Anatomy of Mountain Ranges*, J. P. Schaer and J. Rodgers (Editors), Princeton University Press, Princeton, New Jersey, 277–293.

Tanaka, H., C.-Y. Wang, W.-M. Chen, A. Sakaguchi, K. Ujiee, H. Ito, and M. Ando (2002). Initial science report of shallow drilling penetrating into the Chelungpu fault zone, Taiwan, *Terr. Atmospher. Ocean. Sci.* **113,** 227– 251.

Van der Pluijm, B. A., C. M. Hall, P. J. Vrolijk, D. R. Pevear, and M. C. Covey (2001). The dating of shallow faults in the Earth's crust, *Nature* **412,** 172–175.

Vrolijk, P., A. Fisher, and J. Gieskes (1991). Geochemical and geothermal evidence for fluid migration in the Barbados accretionary prism (ODP leg 110), *Geophys. Res. Lett.* **18,** 947–950.

Vrolijk, P., and B. A. Van der Pluijm (1999). Clay gouge, *J. Struct. Geol.* **21,** 1039–1048.

Wald, D. J., and T. H. Heaton (1994). Spatial and temporal distribution of slip for the 1992 Landers, California, earthquake, *Bull. Seism. Soc. Am.* **84,** 668–691.

Wang, C., T. H. Huang, I. C. Yen, S. L. Wang, and W. B. Cheng (2000). Tectonic environment of the 1999 Chi-Chi earthquake in central Taiwan and its aftershock sequence, *Terr. Atmos. Ocean. Sci.* **11,** 661–678.

Yu, S. B., L. C. Kuo, Y. J. Hsu, H. H. Su, C. C. Lui, C. S. Hou, J. F. Lee, T. C. Lai, C. C. Liu, C. L. Liu, T. F. Tseng, C. S. Tsai, and T. C. Shin (2001). Preseismic deformation and coseismic displacements associated with the 1999 Chi-Chi, Taiwan, earthquake, *Bull. Seism. Soc. Am.* **91,** 995–1912.

Appendix A

Description of the Fengyuan Drill Site, Northern Region

A 450-m-long core was drilled through the fault near the city of Fengyuan from November 2000 through January 2001 (Fig. 1). Groundmat Construction Company from Taipei, Taiwan performed the drilling using a triple tube coring system. Core was taken directly from the core barrel and logged using a standardized logging sheet. Logging from 0 to 350 m (268 m TVD) of the core was performed by R. H. and Z. K. S. on the site during drilling (25 November 2000–12 January 2001). Logging of the core from 350 to 450 m depth (268–345 m TVD) was performed by R. H. in the laboratory after the completion of drilling; the core was housed at National Central University Logging recorded the lithology, structures (depth, fracture type, width, orientation relative to core axis, fracture density, fracture fill, and other notes) and relevant drilling activities (driller comments on hardness, speed of drilling, fluid circulation or loss, etc.). Core dimensions were 1.5 m in length and 6.3 cm in diameter. All logs recorded depths of structures in the core to within 0.01 m. Depths were based on the surface of the drillhole (0 m) and calibrated to the driller's depth during drilling. Core recovery was excellent with the exception of two, 5-m-long sections at 130 m and 230 m core depth, which were lost. These sections consisted of well-sorted, fine-grained, poor/moderately lithified sandstone that liquefied during drilling and therefore was not recoverable. The core was usually saturated with drilling fluids, so water content was not recorded as an *in situ* observation of fault properties.

At 327.6 m core depth (250 m TVD), a 1.5-m-thick gouge zone is encountered that corresponds to the base of the fracture zone with the highest fracture density (Fig. 5). Additionally, an anomalous, thin (7 mm), dark gray, plastic, striated clay zone is present at the base of this 1.5-m-thick brecciated zone (Fig. 4). The clay zone is located along a naturally parted surface in the core. Slickenlines on the surface indicate a 40° rake down from the south, consistent with left-lateral movement in addition to thrusting in the region. These dip and slickenline data agree with surface rupture data from the area (Lin *et al.*, 2001; CGS, 2002). The striated parted surface is unique within the core, is associated with the largest damage zone (30–50 m thick), and is associated with the highest fracture density in the core. Therefore, we interpret the rupture at 327.6 m as the primary fault surface of the 1999 earthquake.

The primary rupture surface of the fault was confined to bedding within the Kuechulin Formation, based on biostratigraphy (Huang *et al.*, 2002). No age determinations have been completed on the core, so the relative ages of the siltstone and shale across the fault are unknown, but there is nothing to suggest that the rocks are not in normal stratigraphic sequence across the fault. The surface rupture shows approximately 7–10 m of slip (J. C. Lee, personal comm., 2000), with Kuechulin Formation sandstone in both the hanging wall and footwall, consistent with a bed-parallel rupture.

The core was drilled at a 50° angle to the ground surface. This meant the core depth is greater than the TVD beneath the ground (Fig. 3), but also that the angled drillhole provided a nearly perpendicular (true thickness) transect through the 53°-dipping fault (Fig. 3). The core was oriented by aligning bedding in the core with surface outcrops (Figs. 3, 11). Bedding dips in the core (average: 58°) correlated well with hanging-wall (average: 56° ± 20°) and footwall

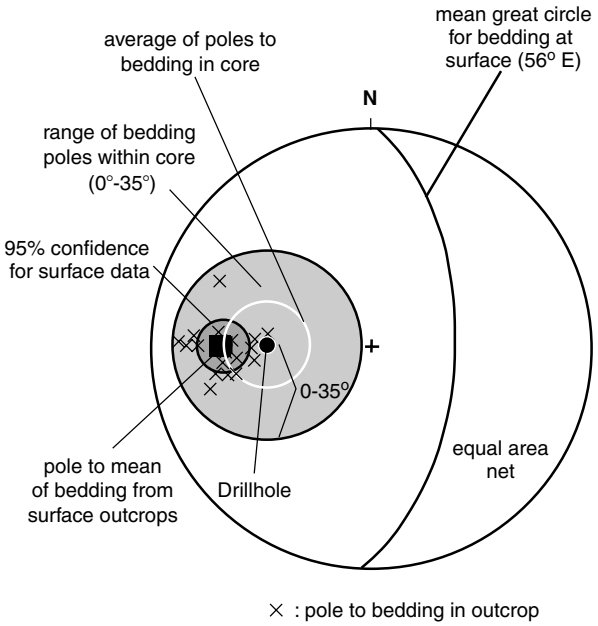

Figure 11. Lower hemisphere stereonet determination of bedding dips within the core. Bedding in the core ranged from 55° to 90°, measured from parallel to the 50° west-dipping core, with an average of 71° and a standard deviation of 7.8°. Surface outcrop dips ranged from 39° to 76° with an average of 56° (pole 34°) and standard deviation of 9.8. The large gray circle indicates the range of the poles to bedding dips (0° to 35°) in the 50°-dipping core. The average of these poles is shown as the white circle. Poles to bedding in outcrop (black crosses) are plotted over the core results. The results indicate that the bedding dips measured in surface outcrops align with the bedding measured in the core in only one, unique position (black square). This indicates that the dips in the core correspond to the surface dips of 56° east.

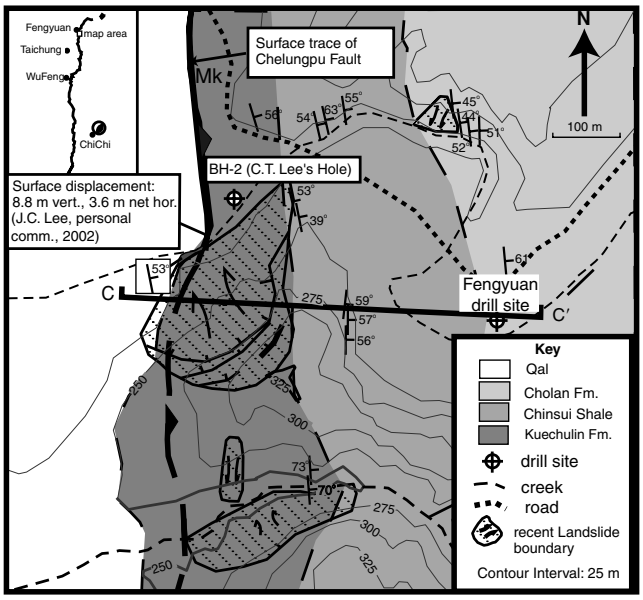

Figure 12. Geologic map of the northern drill site showing local stratigraphy. The inset sketch at the upper left shows the location of the map on the 90-km-long fault trace. The strike and dip of local outcrops are shown. The rupture trace of 1999 earthquake is the thick black line, which is dashed where approximated on the hillslope. Teeth are on the hanging wall. Thin dashed lines indicate streams flowing toward the west. The location of cross section CC′ (Fig. 3) is indicated.

(average: 53° ± 6°) dips at the surface (Fig. 12), indicating that bedding dips were consistent to at least 345 m vertical depth.

The drilled core sampled mudstone and sandstone typical of the Chinsui Shale and Kuechulin Formation, respectively. Both units are interpreted as shallow marine facies (Covey, 1984). Mudstone and sandstone in the core are damp to wet, moderately consolidated, and moderately hard and weak. The mudstone is dark gray with intense bioturbation. Sandstone beds are yellow to tan, fine to medium grained, and generally less consolidated than the mudstone. The contact between the formations is gradational and was interpreted at approximately 220 m core depth from a change from massive mudstone above (Chinsui Shale) to interbedded mudstone and sandstone below (Kuechulin Formation) (Fig. 3). Huang *et al.* (2002) determined this same contact using biostratigraphy markers in the core. Sandstone and mudstone are often interbedded with less than 1-cm-thick laminations (Fig. 13a). Cross-beds, bioturbation, coal, and shell fragments are typical. The sandstone beds and burrows are often calcareous, but the massive mudstone units are generally not. Thin sections show the sedimentary and structural features of the formations within the core (Fig. 14). The Kuechulin Formation consists of interbedded mudstone and fine sandstone with intense bioturbation (Fig. 14a), minor cross-bedding, and some imbrication of clasts along bedding planes. The sandstone and mudstone contain subangular clasts (immature) that are matrix supported. This matrix makes up 20%–30% of the rock based on qualitative analysis of the thin sections. Compositionally, the rocks are quartz rich with less than 5% lithic fragments.

Fractures in the core generally are filled with angular siltstone clasts up to 4 cm in maximum diameter suspended in light gray, clay-silt matrix (Fig. 13d). The matrix consists of massive, clay-rich mudstone with no sedimentary structures (Fig. 14c,d). This fill is 75% fine-grained matrix with 25% silt and sand grains incorporated from the protolith. Silt and clay within the fractures are very soft, moderately plastic, and usually very wet relative to the host rock. Some minor foliation is apparent in the matrix, but generally the silty clay in the fractures shows random grain sorting and alignment (Fig. 14b–d). Brecciated clasts are subangular, show little rotation (Fig. 14b,c), are calcite cemented, and display sharp boundaries with the fracture matrix. Clasts of mudstone are rare in the brecciated zones, implying the sandstone may be stronger than the mudstone in order to exist as

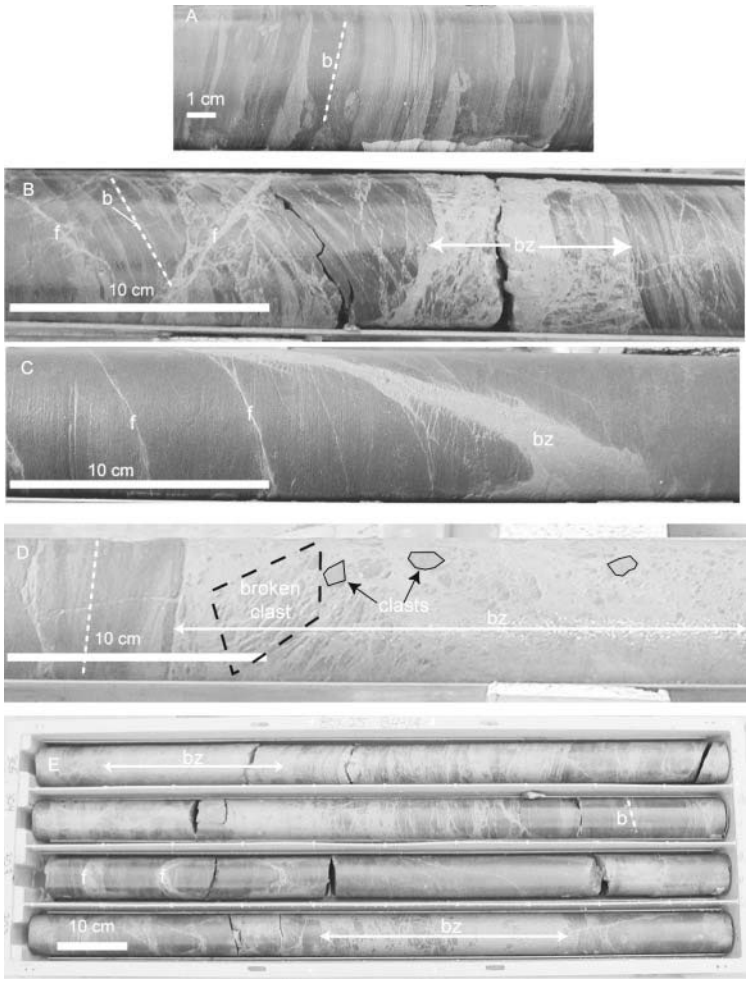

Figure 13. Typical core lithology and structures: b, bedding (dashed lines indicate dip in core); f, fracture; bz, brecciated zone; some clasts are outlined. (a) Thinly laminated, bioturbated mudstone within the Chinsui Shale at 234 m. (b) Intense fracturing cutting beds in the Chinsui Shale at 221.5 m. (c) Fractured Kuechulin Formation at 283 m in core. (d) Upper end of 30 cm brecciated zone from 239 m in core. The fracture contact is sharp and bed parallel. Clasts are outlined in black, and the dashed black line indicates a clast that is currently breaking up. (e) Core box from 301 to 305 m in the core, showing fractures, brecciated zones, and undeformed shale of the Kuechulin Formation.

individual clasts. Clasts make up approximately 10%–50% of the brecciated zones, and clast size scales up with fracture width. There is very little evidence for shear within the fractures, although small (<1 cm) offsets are apparent across some fractures. Fractures vary from irregular to planar and less than 0.001 to 1.5 m in width, and they are filled with dark to light gray clay or silt with brecciated clasts (Fig. 13b,c). That is, smaller clasts are found in smaller width brecciated zones. Fractures, including brecciated zones, frequently occur parallel to bedding (Fig. 13d). Although the fractures are texturally distinct from the protolith, X-ray diffraction analysis (Appendix B) of the core samples indicates that the fractures are compositionally indistinct from the protolith.

The density of fractures varies along the linear transect formed by the drill core. Fracture density is determined using two different methods. Method A involves determining the spatial percentage occupied by fractures within a 5-m section of core. These percentages are then plotted for a 5-m bin size for the entire core length (Fig. 5a). All fractures encountered in the core are used in this method. Method B quantifies the density of all fractures greater than 4 cm width per 5-m bin size. This fracture width is chosen arbitrarily for our analysis to eliminate any bias that might be introduced by including smaller fractures in the histogram. Both methods produce similar results, with the largest density of fractures occurring immediately above 327 m (Fig. 5a,b), the interpreted location of the fault rupture surface. Fracture density begins to increase approximately 30 m above the primary rupture surface and abruptly falls off below the fault. This asymmetry appears to be characteristic of the Chelungpu fault in the northern region.

Other areas of increased fracture density are also observed in the core. Method A shows that fracture density increases at 150, 300, and 400 m core depth. Method B shows abrupt increases in the density of fractures at 150, 250, 300, and 400 m depth in the core. All areas of increased fracture density are associated with brecciated zones greater than 0.5 m thick at their base. These zones may define smaller, subsidiary faults to the main Chelungpu fault. From the orientation of these structures with respect to bedding in the core, we can say that these subsidiary faults are synthetic to the main fault. Fracture density consistently increases above the widest fractures (>0.5 m thick) and abruptly drops off below these fractures, producing a similar asymmetry to the fracture pattern around the primary rupture surface.

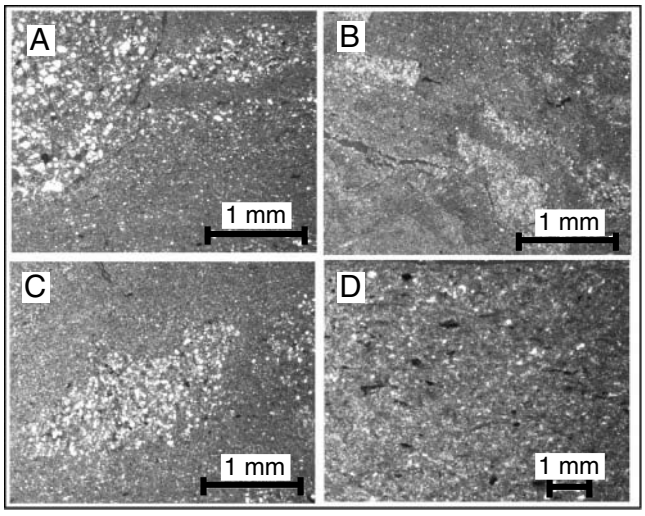

Figure 14. Thin-section photomicrographs of core samples: (a) Typical laminated mudstone and siltstone protolith. This is from the Kuechulin Formation at 328 m core depth, less than 2 m into the footwall of the primary rupture surface. There is very little deformation in the sample. Top of photo is up. The massive sandstone in the upper right is an undeformed, sand-filled burrow and is lithologically typical of the sandstone encountered in the core. (b) Breccia clasts in clay-rich mudstone matrix from a 6-cm fracture (brecciated zone) at 321.4 m. There are very few structural textures. (c) Brecciated sandstone clast from a 28-cm brecciated zone at 322.55 m. Notice the lack of foliation in the surrounding clay-rich matrix. (d) Typical matrix in a 1.5-m brecciated zone at 326.45 m in the core, 20 cm above the primary rupture. The matrix consists of massive clay-rich mudstone with less than 15% silt clasts. Minor foliation and no sedimentary structures are apparent.

Appendix B

Takeng Site Description: Northern Region

The fault zone was investigated in detail at a temporarily excavated locality near the town of Takeng in the Tali River, just north of Taichung and 6 km due south of the Fengyuan drill site (Fig. 1). Here, the fault is oriented 320° and dips 48° east across a river channel, subparallel to bedding (strike, due north; dip, 40°–66° east) (Fig. 6). Net displacement at this location reached 7.3 m during the earthquake (CGS, 1999).

The excellent fault exposure at Takeng was mapped and samples collected during December 2000. A distinctive, 20-cm-thick, dark gray clay gouge lies at the fault (siltstone/conglomerate) contact (Fig. 6). The gouge changes across a sharp contact from dark gray (derived from shale) to reddish brown (derived from conglomerate) at approximately 15 cm into the gouge from the hanging wall (Fig. 7a). The siltstone in the hanging wall within approximately 30 m of the gouge is intensely fractured, and bedding is indistinguishable. This is interpreted as the damage zone of the fault that may record the effects of accumulated slip over much of the fault history (Chester and Logan, 1986; Caine *et al.*, 1996). Beyond this zone, fracture density decreases and bedding is apparent. At least two synthetic faults with less than 1 m vertical displacement are apparent in the hanging wall. Very little deformation is apparent in the footwall. The subparallel geometry of the fault to the hanging-wall bedding implies that

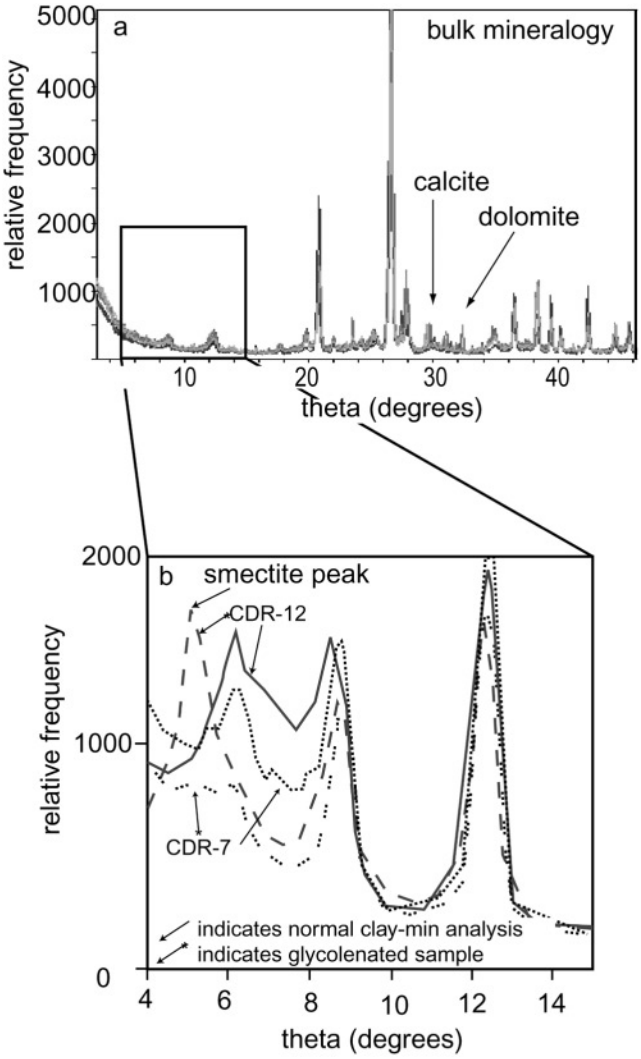

Figure 15. X-ray diffraction results from samples from the Takeng fault outcrop. (a) Bulk mineralogy of all samples collected in a 100-m transect through the hanging wall into the fault. All sample runs are superimposed on each other. Analysis indicates the bulk mineralogy of the samples remains the same along a transect into the fault zone. Sample locations are shown on Figure 10. (b) Close-up of clay mineralogy for samples CDR-7, located ~1 m from the fault gouge (dotted black line), and CDR-12, located ~100 m from the fault gouge (solid black line). The glycolenated runs are shown as the dashed versions of the dotted and solid lines, respectively. Analysis indicates that smectite is a dominant clay mineral in the protolith, but it is not apparent in the sample near the fault.

bedding planes may have acted as a guide for the rupture in the near surface, contributing to the large offsets in the northern region.

X-ray diffraction analysis of fault rocks indicates a change in clay mineralogy between the fault-related rocks and undeformed siltstone away from the fault gouge in the hanging wall. The siltstone 100 m into the hanging wall from the fault gouge contained primarily smectite, illite, amesite, and kaolinite (Fig. 15b). Within the damage zone (<30 m from fault gouge) and in the fault core, the dominant clay minerals are vermiculite, illite, amesite, and kaolinite (Fig. 15b). Other than this clay variability, the rocks from the undeformed protolith and the frature fill (matrix and siltstone clasts) near the fault show identical bulk mineralogy (Fig. 15a). The compositional signature of decreasing smectite toward the fault is consistent with other localities along the Chelungpu fault (Liao *et al.*, 2002) and indicates a fault genesis for the clay. Similar signatures showing a decrease in smectite toward fault zones have been observed in thrust faults in the Canadian fold-and-thrust belt (Vrolijk and Van der Pluijm, 1999; Van der Pluijm, 2001) and the Barbados accretionary prism (Bekins *et al.*, 1994; Vrolijk *et al.*, 1991). These studies indicate the change in clay mineralogy may be attributable to fluid flow in the fault zone inducing a smectite–illite conversion along the fault, and this change may facilitate slip localization in zones of clay alteration (Vrolijk and Van der Pluijm, 1999).

Utah State University
4505 Old Main Hill
Logan, Utah 84322-4505

Manuscript received 23 August 2001.